

$\text{Os}(\text{H})(\text{Cl})(\text{CO})(\text{PPh}_3)_3$,⁴⁸ $\text{Rh}(\text{COD})(\text{PPh}_3)_2^+$,⁴⁸ $\text{Ir}(\text{COD})(\text{PPh}_3)_2^+$,⁴⁸ and $\text{Cp}^*\text{Rh}(\text{NCMe})_3^{2+}$.⁴⁹ In fact, the $\text{Cp}^*\text{Rh}(\text{NCMe})_3^{2+}$ -catalyzed deuteration (D_2) of BT gives specifically the *cis*-dideuteriobenzo[*b*]thiophene; this is the stereochemistry predicted by the mechanism in Scheme III. Thus, the mechanism that was proposed for this reaction by Fish and co-workers⁴⁹ is supported by the characterization of $\text{Cp}'(\text{CO})_2\text{Re}(2,3-\eta^2\text{-BT})$.

This olefin hydrogenation mechanism is also likely to be involved in the conversion of BT to DHBT on heterogeneous catalysts. It allows one to account for the relative rates of hydrogenation and HDS of methyl-substituted benzo[*b*]thiophenes on Co-Mo/ Al_2O_3 catalysts. These rates decrease with increasing methyl substitution in the order $\text{BT} > 2\text{-MeBT} > 3\text{-MeBT} > 2,3\text{-MeBT}$.^{7a,i,j} This trend can be readily explained by the results of our rhenium studies reported herein, which show that 2,3-methyl substitution favors $\eta^1(\text{S})\text{-BT}$ coordination and decreases the amount of the 2,3- η^2 form. On an HDS catalyst, a lower concentration of methyl-substituted (2,3- η^2)-BT

would reduce the overall rate of hydrogenation.

It is also interesting to note that the equilibrium between the 2,3- η^2 and $\eta^1(\text{S})$ forms is affected by the electron density on the metal, which we reduced by replacing Cp^* with Cp in the $\text{Cp}'(\text{CO})_2\text{Re}(\text{BT})$ complexes (Scheme II). On a catalyst, the electron richness of a metal site would be affected by its oxidation state as well as the other groups attached to it. Since 2,3- η^2 coordination is favored by an electron-rich metal center, one would expect metal catalysts in low oxidation states to be the most effective catalysts for the hydrogenation of BT to DHBT.

Acknowledgment. We are grateful to Dr. Lee M. Daniels of the Iowa State University Molecular Structure Laboratory for attempting to determine the structure of 1a. We also thank Professor R. A. Jacobson for permission to use his X-ray facilities for the structural determination of 4.

Supplementary Material Available: For 4, full tables of bond distances, bond angles, and positional and thermal parameters (5 pages). Ordering information is given on any current masthead page.

OM920125F

(48) Sánchez-Delgado, R. A.; González, E. *Polyhedron* 1989, 8, 1431.

(49) Fish, R. H.; Baralt, E.; Smith, S. J. *Organometallics* 1991, 10, 54.

Incorporation of Trialkylsilyl and Trialkylstannyl Groups into Ruthenium Carbonyl Clusters. Carbonyl Substitution versus Trialkylsilane or Trialkylstannane Elimination in These Clusters

Javier A. Cabeza,^{*1a} Angela Llamazares,^{1a} Víctor Riera,^{1a} Small Trikl,^{1b} and Lahcène Ouahab^{1b}

Departamento de Química Organometálica, Universidad de Oviedo, 33071 Oviedo, Spain, and Laboratoire de Cristalchimie, Université de Rennes I, URA-CNRS 254, Avenue du Général Leclerc, 35042 Rennes Cédex, France

Received January 3, 1992

The clusters $[\text{Ru}_3(\mu\text{-H})(\mu_3\eta^2\text{-ampy})(\text{PPh}_3)_n(\text{CO})_{9-n}]$ ($n = 0$ (1), 1 (2), 2 (3); Hampy = 2-amino-6-methylpyridine) react with HSiEt_3 to give the oxidative substitution products $[\text{Ru}_3(\mu\text{-H})(\mu_3\eta^2\text{-ampy})(\text{SiEt}_3)(\text{PPh}_3)_n(\text{CO})_{8-n}]$ ($n = 0$ (4a), 1 (5a), 2 (6a)). Similar reactions of 1-3 with HSnBu_3 afford $[\text{Ru}_3(\mu\text{-H})(\mu_3\eta^2\text{-ampy})(\text{SnBu}_3)(\text{PPh}_3)_n(\text{CO})_{8-n}]$ ($n = 0$ (4b), 1 (5b), 2 (6b)). In all cases, (a) the added hydride spans a metal-metal edge adjacent to that supported by the bridging amido group, (b) the SiEt_3 or SnBu_3 ligands occupy an equatorial site on the Ru atom bound to the two hydrides, being *trans* to the hydride which spans the same edge as the amido group, and (c) in the compounds containing PPh_3 ligands, these ligands occupy equatorial positions, *cis* to hydrides, on the Ru atoms bound to only one hydride. The reactions of 4a and 5a with PPh_3 produce the elimination of HSiEt_3 , rendering the complexes 2 and 3, respectively; however, similar reactions of the tin-containing compounds 4b and 5b afford the substitution products 5b and 6b, respectively. The compounds have been characterized by infrared and ^1H , ^{13}C , and ^{31}P NMR spectroscopies and, in the case of 4a by X-ray diffraction. Crystal data for 4a: monoclinic, space group $P2_1/n$, $a = 10.849$ (8) Å, $b = 20.809$ (4) Å, $c = 12.049$ (8) Å, $\beta = 98.21$ (5)°, $V = 2692$ (2) Å³, $Z = 4$, $\mu(\text{Mo K}\alpha) = 17.17$ cm⁻¹, $R = 0.048$, $R_w = 0.053$ for 2036 reflections and 287 variables.

Introduction

Organosilanes and organostannanes are widely used in metal-catalyzed hydrosilylation² and hydrostannation³ reactions. However, little attention has been paid to metal carbonyl clusters as catalyst precursors in such reactions.²⁻⁴

Concerning ruthenium, the trinuclear clusters $[\text{Ru}_3(\text{CO})_{12}]$ and $[\text{Ru}_3(\mu\text{-H})(\text{CO})_{11}]^-$ have been reported as catalyst precursors for the dehydrogenative silylation^{4c} and hydrosilylation^{4d} of olefins, respectively. In the latter process, the anionic cluster $[\text{Ru}_3(\mu\text{-H})(\text{CO})_{11}]^-$ reacts with triethylsilane to give the trinuclear derivative $[\text{Ru}_3(\mu\text{-H})$

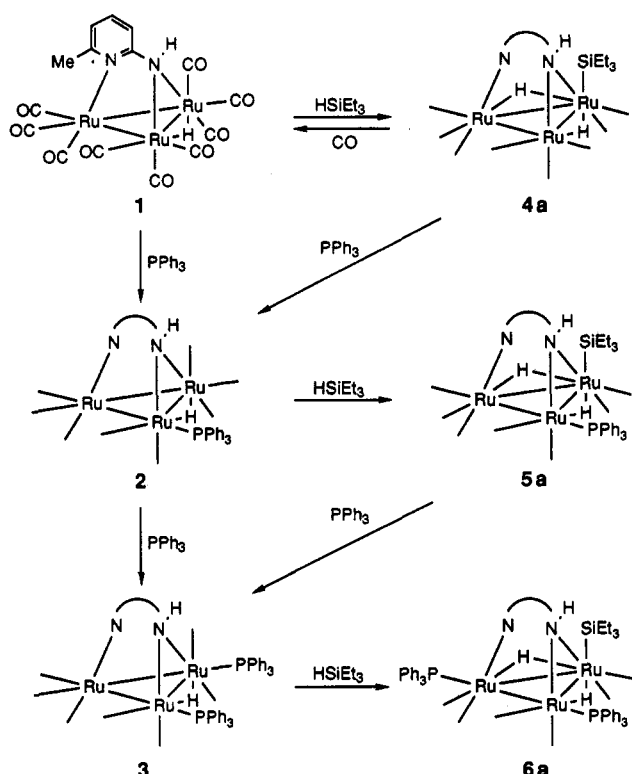
(1) (a) Universidad de Oviedo. (b) Université de Rennes I.

(2) See, for example: Ojima, I. In *The Chemistry of Organic Silicon Compounds*; Patai, S., Rappoport, Z., Eds.; John Wiley and Sons: New York, 1989; Chapter 25, pp 1479-1526.

(3) (a) Pereyre, M.; Quintard, J. P.; Rahm, A. *Tin in Organic Synthesis*; Butterworths: London, 1986. (b) Stille, J. K. *Angew. Chem., Int. Ed. Engl.* 1986, 25, 508. (c) Zhang, H. X.; Guibé, F.; Balavoine, G. *J. Org. Chem.* 1990, 55, 1857 (and references cited therein).

(4) (a) Gladfelter, W. L.; Roessel, K. J. In *The Chemistry of Metal Cluster Complexes*; Schriver, D. F., Kaesz, H. D., Adams, R. D., Eds.; VCH Publishers: New York, 1990; Chapter 7, pp 329-365. (b) Ojima, I.; Donovan, R. J.; Clos, N. *Organometallics* 1991, 10, 2606 (see also references cited therein). (c) Seki, Y.; Takeshita, K.; Kawamoto, K.; Murai, S.; Sonoda, N. *Angew. Chem., Int. Ed. Engl.* 1980, 19, 928. (d) Süß-Fink, G.; Reiner, J. *J. Mol. Catal.* 1982, 16, 231. (e) Süß-Fink, G. *Angew. Chem., Int. Ed. Engl.* 1982, 21, 73.

Scheme I



(SiEt₃)₂(CO)₁₀]⁻, which has two σ -bound SiEt₃ ligands;^{4e} however, the reactions of [Ru₃(CO)₁₂] with trialkylsilanes and trialkylstannanes have been shown to lead to the break up of the trinuclear structure, affording bi- and mononuclear derivatives.⁵ A very recent report has provided examples of trialkoxysilyl groups attached to triosmium clusters, showing that the alkoxy fragments can also coordinate to metals through their oxygen atoms, i.e. as in [Os₃(μ -H)(μ_3 , η^3 -Si(OEt)₃)(CO)₉].⁶

We now report some examples of trialkylsilyl and trialkylstannyl ligands coordinated to neutral ruthenium clusters. We also describe some reactions which prove that hydrido-stannyl complexes are more stable than hydrido-silyl derivatives toward the elimination of trialkylstannane or trialkylsilane. As a starting ruthenium carbonyl cluster, we have used the complex [Ru₃(μ -H)(μ_3 , η^2 -ampy)(CO)₉]^{7,8} (1) (Hampy = 2-amino-6-methylpyridine) because, as reported in previous works,⁹⁻¹² the face-bridging ampy ligand has proved to hold the metal atoms firmly, preventing cluster degradation. The products have been characterized by ¹H, ¹³C, and ³¹P NMR spectroscopies and other analytical methods and, in one case (namely, the cluster [Ru₃(μ -H)₂(μ_3 , η^2 -ampy)(SiEt₃)(CO)₈], by a crystal structure determination.

(5) (a) Knox, S. A. R.; Stone, F. G. A. *J. Chem. Soc. A* 1969, 2559. (b) Vancea, L.; Graham, W. A. G. *Inorg. Chem.* 1974, 13, 511.

(6) Adams, R. D.; Cortopassi, J. E.; Pompeo, M. P. *Inorg. Chem.* 1991, 30, 2960.

(7) Andreu, P. L.; Cabeza, J. A.; Riera, V.; Jeannin, Y.; Miguel, D. *J. Chem. Soc., Dalton Trans.* 1990, 2201.

(8) (a) Lujan, N.; Laurent, F.; Lavigne, G.; Newcomb, T. P.; Liimata, E. W.; Bonnet, J. *J. Am. Chem. Soc.* 1990, 112, 8607. (b) Lujan, N.; Laurent, F.; Lavigne, G.; Newcomb, T. P.; Liimata, E. W.; Bonnet, J. *J. Organometallics* 1992, 11, 1351.

(9) Andreu, P. L.; Cabeza, J. A.; Riera, V.; Bois, C.; Jeannin, Y. *J. Chem. Soc., Dalton Trans.* 1990, 3347.

(10) Andreu, P. L.; Cabeza, J. A.; Pellighelli, M. A.; Riera, V.; Tiripicchio, A. *Inorg. Chem.* 1991, 30, 4611.

(11) Andreu, P. L.; Cabeza, J. A.; Riera, V. *Inorg. Chim. Acta* 1991, 186, 225.

(12) Andreu, P. L.; Cabeza, J. A.; Cuyás, J. L.; Riera, V. *J. Organomet. Chem.* 1992, 427, 363.

Table I. Selected IR Data

compd	$\nu(\text{CO})$, ^a cm ⁻¹
4a	2080 (s), 2047 (vs), 2017 (vs), 1999 (s), 1987 (m), 1951 (m)
4b	2080 (s), 2048 (vs), 2012 (vs), 2000 (m, sh), 1983 (m), 1948 (m)
5a	2058 (vs), 2009 (vs), 2002 (vs), 1986 (m), 1944 (s)
5b	2060 (s), 2009 (vs, br), 1999 (s, sh), 1987 (m), 1972 (w, sh), 1942 (s)
6a	2021 (s), 2002 (vs), 1978 (m), 1946 (s), 1937 (m)
6b	2020 (vs), 1997 (vs), 1980 (m), 1951 (m), 1933 (m)

^aIn THF solution. Abbreviations are as follows: s = strong, m = medium, w = weak, v = very, br = broad, sh = shoulder.

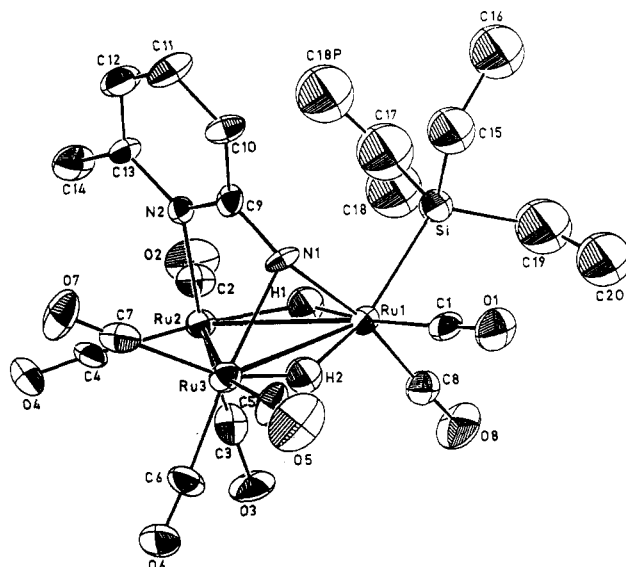
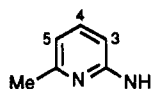


Figure 1. ORTEP drawing of [Ru₃(μ -H)₂(μ_3 , η^2 -ampy)(SiEt₃)(CO)₈] (4a) with atoms shown as 30% probability ellipsoids. C18 and C18P are the two statistically occupied sites for this methyl group.

The potential applications of the compounds described herein as catalyst precursors in reactions involving silanes, stannanes, and organic substrates are currently under investigation in our laboratories.

Results and Discussion

Synthesis and Spectroscopic Characterization. The pale-yellow, air-stable, trinuclear cluster [Ru₃(μ -H)₂(μ_3 , η^2 -ampy)(SiEt₃)(CO)₈] (4a) (Scheme I) could be efficiently prepared by treatment of [Ru₃(μ -H)(μ_3 , η^2 -ampy)(CO)₉] (1) with HSiEt₃. Although the reaction proved to be very slow at room temperature, it was complete within minutes in refluxing THF, dichloromethane, or 1,2-dichloroethane. Its IR spectrum (Table I) shows the $\nu(\text{CO})$ absorptions slightly shifted to higher wavenumbers than those of complex 1,⁷ as expected for a higher formal oxidation state of the metal atoms. Its ¹H NMR (Table II) clearly indicates the incorporation of a new hydride and one SiEt₃ group to the original cluster. The number of CO ligands was evident from the ¹³C{¹H} NMR spectrum (Table III), which shows eight CO resonances, three of which split with considerable coupling constants in the proton-coupled ¹³C NMR spectrum (Table III). These data indicate that only three CO ligands are trans to hydrides and, therefore, the SiEt₃ group should be in an equatorial site of the cluster in a position trans to a hydride ligand. With all these data it was not possible to precisely locate the SiEt₃ group in the cluster, and thus, an X-ray structure determination (Figure 1), which is discussed below, was carried out.

Table II. Selected ^1H and $^{31}\text{P}\{^1\text{H}\}$ NMR Data^a

compd	$\delta(^1\text{H})$						$\delta(^{31}\text{P})$
	H ³	H ⁴	H ⁵	NH	Me	$\mu\text{-H}$	
4a ^b	6.34 (d)	7.23 (t)	6.63 (d)	3.92 (s)	2.52 (s)	-8.64 (s), -11.84 (s)	
4b ^c	5.79 (d)	6.34 (t)	5.11 (d)	3.42 (s)	2.04 (s)	-8.76 (s, sat), -11.49 (s, sat)	
5a ^b	6.60 (d)	7.16 (t)	5.70 (d)	<i>d</i>	2.60 (s)	-8.50 (d) [8.2], -11.20 (d) [4.7]	41.9 (s)
5b ^c	5.91 (d)	6.52 (t)	5.57 (d)	<i>d</i>	1.99 (s)	-8.50 (d, sat) [8.4], -10.65 (d, sat) [5.4]	41.3 (s)
6a ^c	5.96 (d)	6.67 (t)	5.82 (d)	2.57 (d) [5.0]	2.08 (s)	-7.62 (t) [6.0], -10.28 (dd) [14.1, 6.0]	17.3 (d) [65.5], 36.3 (d) [65.5]
6b ^c	5.88 (d)	6.69 (t)	5.74 (d)	2.63 (d) [5.9]	1.99 (s)	-8.32 (t, sat) [5.6], -10.27 (dd, sat) [14.1, 5.6]	20.64 (d) [61.0], 37.47 (d) [61.0]

^aSpectra recorded at 300 MHz (^1H) or 121.7 MHz (^{31}P), 25 °C; chemical shifts (δ , ppm) relative to SiMe_4 (internal, ^1H) or 85% H_3PO_4 (external, ^{31}P); multiplicities (s = singlet, d = doublet, t = triplet, sat = with tin satellites) in parentheses; coupling constants (Hz) in brackets [$J_{\text{H-H}}$] or braces [$J_{\text{P-P}}$]; coupling constants $J_{\text{H-H}}$ for H³, H⁴, and H⁵ are of ca. 7.4 Hz in all cases. The ^1H resonances of the SiEt_3 , SnBu_3 , and PPh_3 ligands, although confirming the presence of these ligands in the clusters, are noninformative multiplets. ^bIn CD_2Cl_2 . ^cIn C_6D_6 . ^dUnobserved.

Table III. Selected ^{13}C NMR Data^a

compd	$\delta(\text{CO})$	$\delta(\text{ampy})$	$\delta(\text{SiEt}_3 \text{ or SnBu}_3)$
4a	203.6 (d) [27.5], 203.3, 200.0 (d) [4.6], 197.6 (d) [4.8], 196.8 (d) [20.1], 193.3 (d) [9.6], 189.0 (d) [5.2], 184.7	180.1, 160.1, 139.4, 119.8, 111.8, 30.2	12.4, 9.4
4b	202.9 (d) [25.0], 202.7, 200.0 (d) [4.2], 197.1 (d) [5.6], 196.4 (d) [18.7], 193.9 (d) [10.6], 189.1 (d) [5.3], 183.9	179.7, 159.9, 139.2, 119.6, 111.5, 30.1	30.5, 28.0, 13.8, 13.3
5a	206.1 (d) [18.9], 205.8 (dd) [8.4] [4.2], 203.8, 199.9 (dd) [16.6] [6.2], 199.5, 194.4 (d) [10.9], 189.3 (dd) [17.0] [4.7]	179.9, 159.6, 138.2, 118.3, 110.7, 30.1	11.5, 8.9
5b	206.0 (dd) [8.2] [3.3], 205.7 (d) [18.5], 203.4, 199.7 (dd) [15.3] [4.0], 198.9, 195.1 (d) [11.0], 189.5 (dd) [17.2] [2.1]	179.7, 159.6, 138.3, 118.4, 110.7, 29.9	30.1, 27.9, 13.6, 12.6
6b	208.1 (d) [16.1], 207.3 (dd) [5.0, 2.5], 204.9, 203.5 (br), 201.1 (dd) [15.0] [6.0], 194.3 (d) [14.9]	180.8, 160.8, 137.4, 117.8, 110.4, 30.0	30.2, 28.0, 13.8, 12.1

^aIn order to assign all types of couplings, the spectra (CD_2Cl_2 , 75.5 MHz, 25 °C) were recorded in both proton-decoupled and proton-coupled modes; the data given for the carbonyl resonances correspond to the proton-coupled spectra, the other ones are proton decoupled. The resonances of the PPh_3 ligands have not been included. Chemical shifts (δ , ppm) are relative to internal SiMe_4 . Unless otherwise stated all resonances are singlets; other multiplicities are given in parentheses; coupling constants (Hz) are given in brackets [$J_{\text{C-H}}$] or braces [$J_{\text{C-P}}$]. The compound 6a is not soluble enough to allow spectra to be taken.

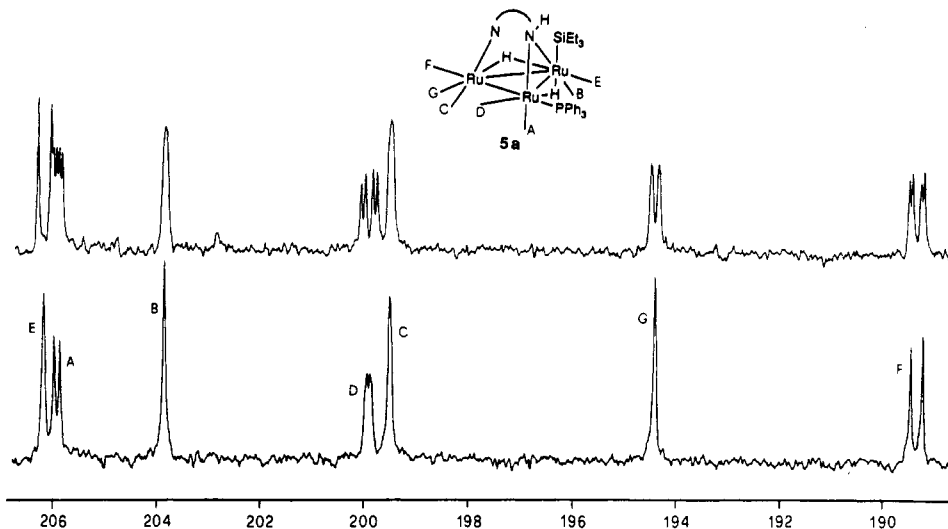


Figure 2. Carbonyl region of the proton-coupled (above) and proton-decoupled (below) ^{13}C NMR spectra (CD_2Cl_2 , 75.5 MHz, 25 °C) of $[\text{Ru}_3(\mu\text{-H})_2(\mu_3, \eta^2\text{-ampy})(\text{SiEt}_3)(\text{PPh}_3)(\text{CO})_7]$ (5a).

The activity and selectivity of homogeneous catalysts are in many cases enhanced by the presence of phosphine ligands.¹³ Thus, we were interested in knowing whether phosphine-substituted derivatives of 1 would behave in the same way as complex 1 in their reactions with triethylsilane.

The cluster $[\text{Ru}_3(\mu\text{-H})(\mu_3, \eta^2\text{-ampy})(\text{PPh}_3)(\text{CO})_8]$ (2) reacted with HSiEt_3 to give $[\text{Ru}_3(\mu\text{-H})_2(\mu_3, \eta^2\text{-ampy})(\text{SiEt}_3)(\text{PPh}_3)(\text{CO})_7]$ (5a) in high yield. The structure we propose for this complex (Scheme I) is based on its spectroscopic data (Tables I–III). Particularly, the carbonyl region of the proton-coupled and proton-decoupled ^{13}C NMR spectra (Figure 2) strongly supports that the coordination sites occupied by the PPh_3 ligand in 2 and the SiEt_3 group in 4a are maintained in 5a. The proton-decoupled spectrum shows three doublets, one with a large coupling constant (17.0 Hz), which we have assigned to

(13) (a) *Homogeneous Catalysis with Metal Phosphine Complexes*; Pignolet, L. H., Ed.; Plenum Press: New York, 1983. (b) Masters, C. *Homogeneous Transition-Metal Catalysis*; Chapman and Hall: London, 1981.

carbonyl F (see assignments in Figure 2), and two with small coupling constants (8.4, 6.2 Hz), which correspond to the CO ligands cis to the phosphine (A and D). The resonances of the axial CO ligands B and C are only slightly broader in the proton-coupled spectrum, while all the others are clearly split, the largest J_{C-H} coupling constants (18.9, 16.6, 10.9 Hz) corresponding to the CO ligands which are trans to hydrides (carbonyls E, D, and G, respectively). The assignments shown in Figure 2 are supported by many other ^{13}C NMR spectra of triruthenium clusters containing the ampy ligand.^{7,9,11,14} It is also known that the *cis*-carbonyl-hydride coupling in trinuclear clusters is very small and many times negligible¹⁵ and that for most trinuclear carbonyl clusters the ^{13}C NMR resonances of the equatorial carbonyls occur at lower frequencies than those of the axial ones (attached to the same metal atom).^{15,16} The high chemical shift of the equatorial carbonyl E in compound 5a must be due to the presence of the two hydrides and the SiEt₃ group on the same ruthenium atom.

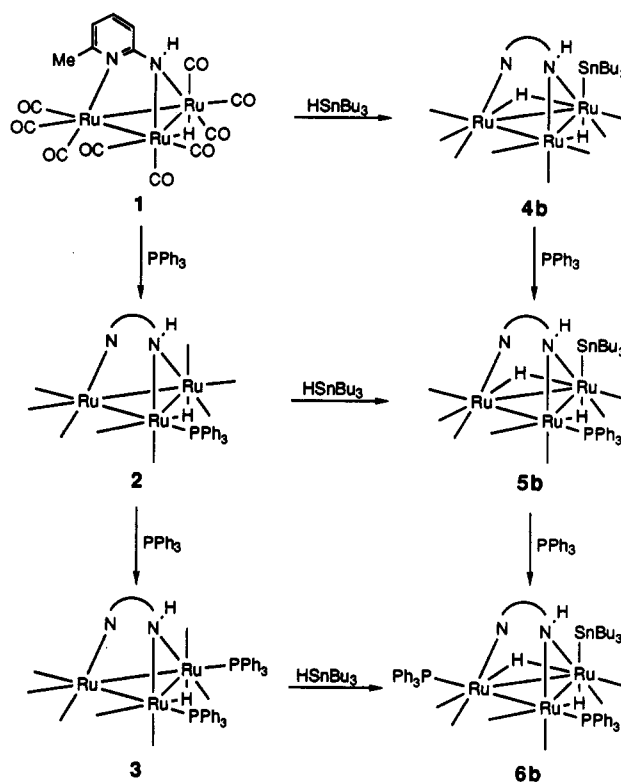
The bis(triphenylphosphine) complex $[Ru_3(\mu-H)(\mu_3, \eta^2\text{-ampy})(PPh_3)_2(CO)_7]$ (3) also reacted smoothly with HSiEt₃ to give $[Ru_3(\mu-H)_2(\mu_3, \eta^2\text{-ampy})(SiEt_3)(PPh_3)_2(CO)_6]$ (6a). The 1H and ^{31}P NMR spectra were particularly useful to propose a structure for this complex. The two hydride resonances of the proton spectrum are coupled to both phosphorus atoms, but the coupling constants are very small (Table II), indicating none of the PPh₃ ligands is trans to hydrides. The $^{31}P\{^1H\}$ NMR spectrum consists of an AX spin system with a coupling constant of 56.5 Hz, typical of two phosphine ligands in a linear arrangement along a metal-metal bond; any other arrangement of two phosphine ligands on different metal atoms would give a much smaller coupling constant.¹⁰ These data strongly support that upon reaction with HSiEt₃ one of the two phosphine ligands of complex 3 moves from its original position to that shown in Scheme I. A related coordination shift of PPh₃ ligand has been reported previously on protonation of complex 3 with HBF₄ to give $[Ru_3(\mu-H)_2(\mu_3, \eta^2\text{-ampy})(PPh_3)_2(CO)_7]BF_4$.¹⁰

In all these reactions only 1 equiv of HSiEt₃ was incorporated into the clusters, even using a large excess of silane. These results contrast with those reported for the anionic complex $[Ru_3(\mu-H)(CO)_{11}]^-$, which reacts with 2 equiv of HSiEt₃ to give hydrogen and the bis-SiEt₃ derivative $[Ru_3(\mu-H)(SiEt_3)_2(CO)_{10}]^-$.^{4e}

The reactions of compounds 1-3 with HSnBu₃ gave the tin-containing derivatives $[Ru_3(\mu-H)_2(\mu_3, \eta^2\text{-ampy})(SnBu_3)(PPh_3)_n(CO)_{6-n}]$ (*n* = 0 (4b), 1 (5b), 2 (6b)) (Scheme II). Their IR and NMR spectra (Tables I-III) are nearly identical to those of the silicon-containing compounds described above, indicating that they have analogous structures. Interestingly, both hydride resonances of their 1H NMR spectra show satellites due to coupling to ^{117}Sn and ^{119}Sn , as expected for hydrides bound to the same ruthenium atom as the SnBu₃ group. Also, the resonances of the ^{31}P NMR spectra do not contain any satellite, suggesting that the phosphine ligands are bound to ruthenium atoms different to that attached to the SnBu₃ group. These data also support the structures we propose for both the silicon- and tin-containing compounds.

Elimination of HSiEt₃ or HSnBu₃ versus CO Substitution Reactions. To compare the reactivity of the

Scheme II



silicon-containing versus the tin-containing complexes, the reactions of triphenylphosphine with all compounds described herein were investigated.

As depicted in Scheme I, the reactions of 4a and 5a with PPh₃ produced the elimination of HSiEt₃, giving 2 and 3, respectively. However, similar reactions with the tin-containing compounds 4b and 5b afforded the carbonyl substitution products 5b and 6b, respectively (Scheme II). Moreover, complex 4b did not react with carbon monoxide (1 atm, refluxing toluene) and complex 6b did not react with triphenylphosphine even in refluxing toluene, whereas complex 4a gave complex 1 upon treatment with carbon monoxide (1 atm) at room temperature and complex 6a gave a mixture of unidentified products upon reaction with triphenylphosphine in refluxing toluene. These reactions demonstrate that the hydrido-stannyl complexes are much more stable than the hydrido-silyl derivatives toward the elimination of trialkylstannane or trialkylsilane.

From a mechanistic point of view, the mild conditions under which many of the reactions described in this and other related⁹⁻¹² works take place suggest that a low-energy path is being used in the transformations. As indicated by Lavigne et al. in related (phenyl(2-pyridyl)amido)ruthenium carbonyl clusters,⁸ the opening of one of the Ru-N arms of the amido bridge would provide a reactive coordinatively unsaturated 46-electron species as a low-energy transition state. Although we have not observed such a bridge opening in any of our neutral complexes containing ampy as a μ_3, η^2 -ligand, it has been observed by others in related anionic complexes; i.e., the complex $PPN[Ru_3\{\mu_3, \eta^2\text{-N(Ph)(C}_5\text{H}_4\text{N)}\}(CO)_9]$ reacts reversibly with carbon monoxide to give $PPN[Ru_3\{\mu_3, \eta^2\text{-N(Ph)(C}_5\text{H}_4\text{N)}\}(CO)_{10}]$ in which the amido group is bound to only one ruthenium atom.⁸

Structural Characterization of $[Ru_3(\mu-H)_2(\mu_3, \eta^2\text{-ampy})(SiEt_3)(CO)_8]$ (4a). The X-ray structure of 4a has been determined by X-ray diffraction (Figure 1). A selection of bond distances and angles is given in Table IV. The cluster consists of a triangle of ruthenium atoms. The

(14) Andreu, P. L.; Cabeza, J. A.; Riera, V. J. *Organomet. Chem.* **1990**, *393*, C30.

(15) See, for example, Ma, A. K.; Einstein, F. W. B.; Johnson, V. J.; Pomeroy, R. K. *Organometallics* **1990**, *9*, 45.

(16) Mann, B. E.; Taylor, B. F. *^{13}C NMR Data for Organometallic Compounds*; Academic Press: New York, 1981.

Table IV. Selected Bond Distances (Å) and Bond Angles (deg) in Complex 4a^c

Bond Distances			
Ru1-Ru2	2.932 (2)	Ru1-Ru3	2.831 (2)
Ru2-Ru3	2.765 (2)	Ru1-Si	2.435 (4)
Ru1-N1	2.15 (1)	Ru2-N2	2.191 (9)
Ru3-N1	2.15 (1)	Ru1-H1	1.7 (1)
Ru1-H2	1.4 (1)	Ru2-H1	1.8 (1)
Ru3-H2	1.9 (1)	Ru1-C1	1.85 (1)
Ru1-C8	1.87 (1)	Ru2-C2	1.93 (1)
Ru2-C3	1.85 (1)	Ru2-C4	1.91 (1)
Ru3-C5	1.93 (2)	Ru3-C6	1.89 (1)
Ru3-C7	1.95 (2)	C-O ^b	1.14 (2)
Bond Angles			
Ru2-Ru1-Ru3	57.30 (4)	Ru1-Ru2-Ru3	59.52 (4)
Ru1-Ru3-Ru2	63.18 (4)	Ru1-H1-Ru2	116 (8)
Ru1-H2-Ru3	116 (8)	Ru2-Ru1-Si	108.0 (1)
Ru3-Ru1-Si	147.2 (2)	Ru1-N1-Ru3	82.4 (4)
Si-Ru1-H1	80 (4)	Si-Ru1-H2	164 (5)
C1-Ru1-H1	166 (5)	C2-Ru2-Ru3	173.8 (4)
N2-Ru2-C3	169.3 (6)	C4-Ru2-H1	173 (4)
C5-Ru3-Ru2	165.3 (5)	N1-Ru3-C6	166.7 (5)
C7-Ru3-H2	156 (4)	N1-Ru1-C8	170.2 (5)

^a Estimated standard deviations in parentheses. ^b Averaged value.

μ_3, η^2 -ampy ligand occupies three axial coordination sites, being linked to the Ru2 atom through the pyridinic nitrogen N2 and to the other two Ru atoms through the exocyclic nitrogen N1. The planes Ru1-N1-Ru3 and that of the pyridine ring are nearly perpendicular to the Ru_3 plane (dihedral angles 92.7 (3)° and 85.4 (3)°, respectively). Two bridging hydrido ligands, H1 and H2, span the Ru1-Ru2 and Ru1-Ru3 edges of the metal triangle. While the hydride H1 is almost coplanar with the Ru_3 plane, the plane Ru1-Ru3-H2 forms a dihedral angle of 84 (8)° with the metal triangle. Although the location of hydrides by X-ray methods has always to be considered cautiously, in our case the X-ray data fit consistently with the NMR data. A SiEt₃ group is coordinated, in an equatorial position, to the Ru1 atom through the silicon atom, being nearly trans to the hydride H2. The ligand shell of the cluster is completed by eight carbonyl ligands, three in axial positions (trans to the nitrogen atoms of the ampy ligand) and five in equatorial positions (two trans to ruthenium atoms and three trans to hydrides).

Overall, this structure reminds us of that of the clusters $[Ru_3(\mu-H)_2(\mu_3, \eta^2\text{-ampy})(CO)_9]^+$ and $[Ru_3(\mu-H)_2(\mu_3, \eta^2\text{-ampy})(PPh_3)(CO)_9]^+$,⁹ in which one CO and one PPh₃ ligand, respectively, formally replace the SiEt₃ group of complex 4a. It is interesting to note that the interatomic distances of 4a are comparable to those in $[Ru_3(\mu-H)_2(\mu_3, \eta^2\text{-ampy})(CO)_9]^+$ and $[Ru_3(\mu-H)_2(\mu_3, \eta^2\text{-ampy})(PPh_3)(CO)_9]^+$ although the latter are cationic species.

Experimental Section

General Procedures. Solvents were dried over sodium diphenyl ketyl (THF, hydrocarbons) or CaH₂ (dichloromethane, 1,2-dichloroethane) and distilled under nitrogen prior to use. All reactions were carried out under nitrogen using standard Schlenk techniques and were monitored by solution IR spectroscopy (carbonyl stretching region). The clusters 1,⁷ 2,⁹ and 3¹⁰ were prepared as described previously; all other reagents were purchased from Aldrich and used as received. Infrared spectra (Table I) were recorded in solution on a Perkin-Elmer FT 1720-X spectrophotometer, using 0.1-mm CaF₂ cells. NMR spectra (Tables II and III) were run with a Bruker AC-300 instrument, using SiMe₄ (internal, ¹H, ¹³C) or 85% H₃PO₄ (external, ³¹P) as standards ($\delta = 0$ ppm). Microanalyses were obtained from the University of Oviedo Analytical Service.

$[Ru_3(\mu-H)_2(\mu_3, \eta^2\text{-ampy})(SiEt_3)(CO)_9]$ (4a). HSiEt₃ (0.5 mL) was added to a solution of complex 1 (146 mg, 0.221 mmol) in

1,2-dichloroethane (8 mL). The initial orange solution was refluxed until the color turned pale-yellow (7 min). The solvent was eliminated under reduced pressure, *n*-pentane (5 mL) added, and the suspension evaporated again to dryness to give complex 4a as a pale yellow solid (152 mg, 93%). Anal. Calcd for C₂₀H₂₄N₂O₈Ru₃Si: C, 31.96; H, 3.22; N, 3.73. Found: C, 31.56; H, 2.93; N, 3.72. This product is soluble in all organic solvents.

$[Ru_3(\mu-H)_2(\mu_3, \eta^2\text{-ampy})(SnBu_3)(CO)_9]$ (4b). A mixture of HSnBu₃ (21 μ L, 0.076 mmol) and complex 1 (50 mg, 0.075 mmol) in THF (10 mL) was stirred at reflux temperature for 7 min to give a pale yellow solution. The solvent was eliminated under vacuum to give a pale yellow oil, soluble in all organic solvents, which could not be crystallized but which was spectroscopically pure (IR, NMR).

$[Ru_3(\mu-H)_2(\mu_3, \eta^2\text{-ampy})(SiEt_3)(PPh_3)(CO)_7]$ (5a). HSiEt₃ (0.5 mL) was added to a solution of complex 2 (63 mg, 0.070 mmol) in THF (10 mL). This solution was refluxed for 25 min and then evaporated to dryness. The oily residue was dissolved in *n*-pentane (5 mL) and the resulting solution evaporated to dryness to give 5a as a yellow solid (55 mg, 81%). Anal. Calcd for C₃₇H₃₉N₂O₇PRu₃Si: C, 45.07; H, 3.99; N, 2.84. Found: C, 45.56; H, 4.13; N, 2.78.

$[Ru_3(\mu-H)_2(\mu_3, \eta^2\text{-ampy})(SnBu_3)(PPh_3)(CO)_7]$ (5b). A mixture of HSnBu₃ (21.5 μ L, 0.077 mmol) and complex 2 (69 mg, 0.077 mmol) in THF (10 mL) was refluxed for 10 min to give a yellow solution. The solvent was removed under reduced pressure and the residue dissolved in *n*-hexane (3 mL). This solution was kept at -20 °C for 15 h to give yellow crystals of 5b (42 mg). The mother liquor was concentrated to 1 mL and kept at -20 °C for 2 days, affording a second crop of yellow crystals (12 mg, overall yield 64%). Anal. Calcd for C₄₃H₅₁N₂O₇PRu₃Sn: C, 44.94; H, 4.43; N, 2.41. Found: C, 45.05; H, 4.52; N, 2.38.

$[Ru_3(\mu-H)_2(\mu_3, \eta^2\text{-ampy})(SiEt_3)(PPh_3)_2(CO)_6]$ (6a). HSiEt₃ (0.5 mL) was added to a solution of complex 3 (45 mg, 0.040 mmol) in 1,2-dichloroethane (10 mL). The initial red solution was refluxed until the color turned orange (45 min). The solvent was removed under reduced pressure and the solid residue washed with *n*-hexane (two 5-mL portions), to give complex 6a as a yellow-orange solid (34 mg, 70%). Anal. Calcd for C₅₄H₅₄N₂O₆P₂Ru₃Si: C, 53.15; H, 4.46; N, 2.30. Found: C, 52.54; H, 4.00; N, 2.07.

$[Ru_3(\mu-H)_2(\mu_3, \eta^2\text{-ampy})(SnBu_3)(PPh_3)_2(CO)_6]$ (6b). A dichloromethane solution (6 mL) of complex 3 (46 mg, 0.041 mmol) and HSnBu₃ (11.5 μ L, 0.041 mmol) was stirred at reflux temperature for 2 h. The IR spectrum of this solution still showed the presence of unreacted starting material 3. The solvent was removed, THF added (5 mL), and the resulting solution refluxed for 30 min. The solvent was again removed and the residue washed with *n*-hexane (1 mL) to give complex 6b as a yellow solid (51 mg, 89%). Anal. Calcd for C₆₀H₆₆N₂O₆P₂Ru₃Sn: C, 51.66; H, 4.77; N, 2.01. Found: C, 51.87; H, 4.90; N, 1.88.

Reaction of Complex 4a with Carbon Monoxide. Carbon monoxide was bubbled, at room temperature, through a solution of complex 4a (31 mg, 0.041 mmol) in THF (10 mL). After 40 min, the IR spectrum of the solution showed the quantitative transformation of 4a into 1.

Reaction of Complex 4a with Triphenylphosphine. A solution of complex 4a (41 mg, 0.055 mmol) in THF (10 mL) was treated with PPh₃ (15 mg, 0.057 mmol). After 1 h, the IR spectrum of the solution indicated that it only contained the complex 2.

Reaction of Complex 5a with Triphenylphosphine. A solution of complex 5a (9 mg, 0.009 mmol) in THF (4 mL) was treated with PPh₃ (3.3 mg, 0.013 mmol). After stirring for 2 h at room temperature, the reaction was incomplete (IR). It was then heated at reflux temperature for 2 min, when the IR spectrum showed the complete transformation of 5a into 3.

Reaction of Complex 4b with Triphenylphosphine. A solution of complex 4b, prepared in situ (as described above) from complex 1 (27 mg, 0.041 mmol) and HSnBu₃ (12 μ L, 0.042 mmol) in THF (6 mL), was treated with PPh₃ (11 mg, 0.042 mmol) at room temperature for 8 h. At this point, the IR spectrum of the solution showed that it only contained the cluster 5b.

Reaction of Complex 5b with Triphenylphosphine. The solution obtained above was treated with PPh₃ (12 mg, 0.046) and the mixture stirred at room temperature for 15 h. Since the IR spectrum of this solution showed no reaction, it was heated at

Table V. Crystallographic and Refinement Data for Complex 4a

formula	C ₂₀ H ₂₄ N ₂ O ₈ Ru ₃ Si
fw	751.72
cryst syst	monoclinic
space group	P2 ₁ /n
a, Å	10.849 (8)
b, Å	20.809 (4)
c, Å	12.049 (8)
β, deg	98.21 (5)
V, Å ³	2692 (2)
Z	4
D _{calcd} , g·cm ⁻³	1.854
cryst size, mm	0.5 × 0.2 × 0.1
radiation (λ, Å)	Mo Kα (0.71073)
monochromator	graphite
temp, K	293
μ(Mo Kα), cm ⁻¹	17.17
scan method	θ-2θ
h, k, l range	0-12, 0-24, ±14
2θ range, deg	2-50
no. of measd rflcns	4784
no. of unique rflcns	4519
no. of rflcns with I ≥ 3σ(I)	2036
R _{int}	0.026
no. of variables	287
R(F) ^a	0.048
R _w (F) ^b	0.053
GOF ^c	1.556
Δ/σ	5.89
Δρ(min, max), eÅ ⁻³	0.887, -0.629

^a $R = \sum(|F_o| - |F_c|) / \sum|F_o|$. ^b $R_w = [\sum w(|F_o| - |F_c|)^2 / \sum w|F_o|^2]^{1/2}$. ^c Goodness of fit (GOF) = $[\sum w(|F_o| - |F_c|)^2 / (N_{obs} - N_{var})]^{1/2}$. $w = 4F_o^2 / [\sigma^2(I) + (0.04|F_o|^2)^2]$.

reflux temperature for 45 min, to give quantitatively the complex 6b (IR identification).

Crystal Data Collection, Solution, and Refinement of the X-ray Structure of 4a. A pale-yellow crystal of compound 4a was mounted on an Enraf-Nonius CAD4 diffractometer, equipped with graphite-crystal-monochromated Mo Kα radiation. The cell dimensions were determined by least-squares refinement from the setting angles of 25 centered reflections in the range 10 < 2θ < 20°. The intensities were collected using the θ-2θ scan method. The measurement of three standard reflections every 60 min revealed no intensity fluctuations. One set of reflections was collected up to 2θ = 50°. The intensities were corrected for Lorentz and polarization effects. No absorption correction was applied. The crystal data are summarized in Table V. The structure was solved by direct methods¹⁷ and successive Fourier difference syntheses and was refined by weighted anisotropic full-matrix least-squares methods. The ethyl carbon atoms of the SiEt₃ group (C15-C20) were refined isotropically. They showed high thermal motions and disorder; in particular, one methyl group was found in two sites (C18 and C18P) with occupancy factors of 0.5. After refinement of positional and anisotropic (β_{ij}) thermal parameters, the positions of the H-atoms were calculated (C-H = 0.96 Å, B = 5 Å²) and included as a fixed contribution to F_c. The bridging hydrides H1 and H2 were observed in Fourier difference syntheses and their positional parameters refined. Scattering factors and corrections for anomalous dispersion were taken from ref 18. The drawing was made with

Table VI. Positional and Equivalent Isotropic Thermal Parameters for Complex 4a^a

atom	x	y	z	B _{eq} , Å ²
Ru1	0.1579 (1)	0.17637 (5)	0.30095 (9)	3.0
Ru2	0.1592 (1)	0.07540 (5)	0.1314 (1)	3.2
Ru3	0.2084 (1)	0.20162 (6)	0.0810 (1)	3.5
Si	0.2305 (4)	0.1293 (2)	0.4837 (4)	4.4
O1	0.198 (1)	0.3055 (5)	0.413 (1)	6.9
O2	0.101 (1)	-0.0602 (5)	0.210 (1)	7.4
O3	-0.1166 (8)	0.1035 (5)	0.0789 (9)	6.0
O4	0.180 (1)	0.0481 (6)	-0.1120 (8)	6.4
O5	0.257 (1)	0.3473 (6)	0.085 (1)	9.8
O6	-0.004 (1)	0.2072 (5)	-0.1090 (9)	6.2
O7	0.399 (1)	0.1645 (6)	-0.0735 (9)	7.5
O8	-0.1043 (9)	0.1680 (6)	0.355 (1)	7.4
N1	0.3308 (9)	0.1807 (5)	0.2330 (9)	3.5
N2	0.3615 (9)	0.0737 (5)	0.1812 (8)	3.0
C1	0.181 (1)	0.2556 (7)	0.371 (1)	4.2
C2	0.128 (1)	-0.0100 (6)	0.183 (1)	4.5
C3	-0.009 (1)	0.0929 (7)	0.097 (1)	4.2
C4	0.174 (1)	0.0579 (7)	-0.022 (1)	4.6
C5	0.240 (1)	0.2930 (8)	0.086 (1)	5.6
C6	0.075 (1)	0.2072 (7)	-0.038 (1)	4.8
C7	0.329 (1)	0.1780 (8)	-0.018 (1)	5.0
C8	-0.005 (1)	0.1719 (7)	0.334 (1)	4.2
C9	0.409 (1)	0.1301 (7)	0.227 (1)	3.4
C10	0.538 (1)	0.1367 (7)	0.264 (1)	4.6
C11	0.615 (1)	0.0854 (9)	0.252 (2)	6.6
C12	0.565 (1)	0.0291 (8)	0.203 (1)	5.9
C13	0.440 (1)	0.0225 (7)	0.168 (1)	4.1
C14	0.387 (2)	-0.0376 (8)	0.119 (2)	6.5
C15*	0.386 (2)	0.164 (1)	0.540 (2)	8.8 (6)
C16*	0.442 (2)	0.136 (1)	0.655 (2)	12.0 (8)
C17*	0.245 (3)	0.034 (1)	0.487 (2)	13.7 (9)
C18*	0.128 (5)	0.007 (3)	0.491 (5)	14 (2)
C18P*	0.366 (6)	0.024 (3)	0.454 (5)	15 (2)
C19*	0.131 (3)	0.145 (1)	0.597 (2)	12.9 (8)
C20*	0.106 (2)	0.207 (1)	0.626 (2)	11.8 (8)
H1*	0.13 (1)	0.100 (7)	0.27 (1)	5.0
H2*	0.10 (1)	0.187 (7)	0.19 (1)	5.0

^a Estimated standard deviation in parentheses. Starred atoms were refined isotropically. $B_{eq} = (4/3) \sum_i \beta_{ij} a_i a_j$.

ORTEP.¹⁹ All calculations were performed on a MicroVAX 3100 computer using the SDP program package.²⁰ Selected bond lengths and angles are given in Table IV; positional atomic coordinates are given in Table VI.

Acknowledgment. We are grateful to the the CICYT (Spain) (Project No. MAT90-0173) and the CNRS (France) for support of this work. We also thank the FICYT (Asturias, Spain) for a postgraduate scholarship to A.L. and Dr. G. Lavigne (CNRS, Toulouse, France) for a preprint copy of ref 8b.

Supplementary Material Available: For 4a, tables of thermal parameters for the non-hydrogen atoms, bond lengths, bond angles, and H-atom coordinates (4 pages). Ordering information is given on any current masthead page.

OM920004F

(18) *International Tables for X-Ray Crystallography*; Kynoch Press: Birmingham, U.K., 1974; Vol. 4.

(19) Johnson, C. K. *ORTEP*; Report ORNL-3794; Oak Ridge National Laboratory: Oak Ridge, TN, 1965.

(20) Frenz, B. A. & Associates Inc. (College Station, TX). *SDP Structure Determination Package*; Enraf-Nonius: Delft, The Netherlands, 1985.

(17) Main, P.; Fiske, S. J.; Hull, S. E.; Jessinger, L.; Germain, G.; Declercq, J. P.; Woolfson, M. M. MULTAN84 a System of Computer Programs for the Automatic Solution of Crystal Structures from X-Ray Diffraction Data. Universities of York (U.K.) and Louvain (Belgium), 1984.